

16 **Abstract**

17 Climate models generally project an increase in the winter North Atlantic Oscillation (NAO)
18 index under a future high emissions scenario, alongside an increase in winter precipitation in
19 northern Europe and a decrease in southern Europe. The extent to which future forced NAO
20 trends are important for European winter precipitation trends and their uncertainty remains
21 unclear. We show using the Multimodel Large Ensemble Archive that the NAO plays a small
22 role in northern European mean winter precipitation projections for 2080-2099. Conversely, half
23 of the model uncertainty in southern European mean winter precipitation projections is
24 potentially reducible through improved understanding of the NAO. Extreme positive NAO
25 winters increase in frequency in most models, coincident with mean NAO changes. These
26 extremes also have more severe future precipitation impacts, largely because of background
27 mean precipitation changes. This has implications for future resilience to extreme positive NAO
28 winters, which already can have severe societal impacts.

29

30 **Plain Language Summary**

31 Variations in atmospheric circulation over the North Atlantic are dominated by the North
32 Atlantic Oscillation (NAO) pattern. A positive NAO phase is associated with a northward shift
33 of the North Atlantic storm track, bringing wetter weather to northern Europe and drier weather
34 to southern Europe. In response to future human-caused increases in greenhouse gas emissions,
35 climate models generally simulate an increase in the winter NAO, alongside an increase in
36 winter precipitation in northern Europe and a decrease in southern Europe. However, it is unclear
37 what role the NAO plays in future European winter precipitation trends. Here we show, using a
38 large number of simulations from different climate models, that the NAO plays a small role in
39 late 21st century northern European winter precipitation changes. Conversely, the NAO plays a
40 sizable role in southern Europe. This is important because it suggests that model-to-model
41 uncertainty in southern European winter precipitation changes could be reduced with improved
42 understanding of the NAO. Winters with a prolonged extremely positive NAO state are generally
43 projected to increase in frequency and have larger precipitation impacts. This has implications
44 for future resilience to these seasonal extremes, which already can have severe societal impacts
45 including flooding and drought.

46 **1 Introduction**

47 The North Atlantic Oscillation (NAO) is the dominant mode of atmospheric circulation
48 variability in the North Atlantic sector and exerts a strong influence on European weather and
49 climate (Hurrell et al., 2003). A positive NAO phase is associated with a stronger eddy-driven jet
50 stream over the North Atlantic and a northward shift of the storm track. In winter, this brings
51 milder and wetter weather to northern Europe, and colder and drier weather to southern Europe.
52 The NAO is associated with the first mode of interannual variability in European winter
53 precipitation (Álvarez-García et al., 2019; Qian et al., 2000; Seager et al., 2020; Zveryaev, 2006).

54 There are significant societal impacts associated with NAO-induced precipitation
55 variability. On interannual timescales, the NAO has a strong influence on precipitation and river
56 flows in the Iberian Peninsula, with consequent impacts on water availability for hydroelectricity
57 production and intensive agriculture (Trigo et al., 2004). Prolonged winter periods with a
58 predominantly positive NAO state are also connected to the occurrence of catastrophic flood
59 events in northern Europe, with significant impacts on flood economic losses (Zanardo et al.,
60 2019).

61 On longer timescales, climate models on average project an increase in the winter NAO
62 index by the late 21st century under a high emissions scenario (McKenna and Maycock, 2021),
63 alongside an increase in winter precipitation in northern Europe and a decrease in southern
64 Europe (Douville et al., 2021; Lee et al., 2021). While future atmospheric circulation change has
65 been highlighted as a contributor to regional precipitation projections and their uncertainty
66 (Deser et al., 2012, 2017; Fereday et al., 2018; Seager et al., 2010, 2014; Shepherd, 2014; Zappa
67 et al., 2015), it is currently unclear the extent to which future forced NAO trends are important
68 for European mean winter precipitation trends and their uncertainty. Furthermore, since extreme
69 NAO winters are commonly associated with severe societal impacts, it is important to determine
70 whether the projected mean positive NAO anomaly by the end of the century under high
71 anthropogenic emissions alters the frequency of extreme positive NAO winters and their
72 associated precipitation impacts.

73 This study aims to determine the role of the NAO for projections of winter mean
74 European precipitation. Specifically, we aim to address:

- 75 1. What role do modelled forced trends in the NAO play in projections of European
76 mean winter precipitation and their uncertainty?
- 77 2. Do models show an increase in the frequency of extreme positive NAO winters in the
78 future?
- 79 3. Do extreme positive NAO winters have more severe precipitation impacts in the
80 future? If so, what role does the NAO play in this (e.g., through changes in the mean
81 NAO)?

82

83 **2 Methods**

84 2.1 Datasets

85 We use the Multimodel Large Ensemble Archive (MMLEA; Deser et al., 2020). The
86 MMLEA contains large (16-100 member) initial-condition ensembles for seven Coupled Model
87 Intercomparison Project Phase 5 (CMIP5) models (Table S1; Hazeleger et al., 2010; Jeffrey et
88 al., 2013; Kay et al., 2015; Kirchmeier-Young et al., 2017; Maher et al., 2019; Rodgers et al.,
89 2015; Schlunegger et al., 2019; Sun et al., 2018). While CMIP5 models may have stronger
90 precipitation biases than higher resolution models (Roberts et al., 2019), the MMLEA dataset has
91 various unique benefits. Initial-condition large ensembles provide a more accurate measure of
92 the forced climate response and larger samples of relatively rare extreme winters. Multimodel
93 large ensembles also allow us to examine structural model uncertainty and the robustness of
94 projections (Maher et al., 2021b).

95 We use historical and Representative Concentration Pathway (RCP) 8.5 simulations from
96 the MMLEA models for the common period 1950-2099. RCP8.5 was chosen because only a
97 small subset of the models is available for other RCPs. The analysis uses monthly mean
98 precipitation and mean sea level pressure (MSLP) data averaged over December to February
99 (DJF).

100 The models are evaluated using observation-based MSLP data from the NOAA-CIRES-
101 DOE 20th Century Reanalysis version 3 (20CRv3; Compo et al., 2011; Slivinski et al., 2019).

102 This longer-term dataset was chosen to minimise the sampling errors associated with short
103 observational records. A 1000-member “Observational Large Ensemble” (Obs LE; McKinnon &
104 Deser, 2018) is also used for this reason, which contains synthetic historical trajectories
105 produced by a statistical model based on observed climate statistics. Observed precipitation data
106 is taken from the E-OBS dataset (Cornes et al., 2018). We evaluate the models against the
107 observations over a historical period common to all datasets (1951-2014; year is for January).

108 All data were regridded onto a common 2° grid using bilinear interpolation for MSLP
109 and a conservative remapping method in Climate Data Operators (Schulzweida, 2021) for
110 precipitation.

111 2.2 Analysis and statistical methods

112 Following Stephenson et al. (2006) and Baker et al. (2018), the NAO index is defined as
113 the difference in area-average MSLP between a southern box (90°W - 60°E , 20°N - 55°N) and a
114 northern box (90°W - 60°E , 55°N - 90°N) in the North Atlantic. McKenna and Maycock (2021)
115 discuss the advantages of this NAO index definition in detail.

116 Historical NAO-precipitation and NAO-MSLP patterns (Figure S1a) are constructed
117 from the regression slopes obtained by regressing historical (1951-2014) timeseries of DJF
118 precipitation and MSLP in each grid-cell onto the NAO index timeseries. All timeseries are
119 linearly detrended. For MMLEA models, the patterns are defined separately for each ensemble
120 member and then the ensemble mean is calculated (Simpson et al., 2020). The NAO-congruent
121 part of a precipitation or MSLP anomaly map is obtained by multiplying the historical NAO-
122 precipitation or NAO-MSLP pattern by the NAO index anomaly.

123 The long-term forced climate response is calculated as the ensemble mean difference
124 between a future period (2080-2099) and a near-present-day period (1995-2014). Precipitation
125 changes are calculated as a percentage of the modelled 1995-2014 climatology. This reduces the
126 influence of model climatological biases: for example, if a model simulates too little
127 precipitation in a region climatologically, it will be unable to simulate a large decrease in
128 precipitation in that region. Since this study concerns the NAO’s role in Europe-wide
129 precipitation projections, we calculate the area-average precipitation change over large areas of

130 northern (45°N-72°N, 10°W-30°E) and southern (32°N-45°N, 10°W-30°E) Europe. These
131 regions are defined based on broad areas of wetting to the north and drying to the south in the
132 multimodel mean MMLEA precipitation projections.

133 95% confidence intervals in a given quantity for a single large ensemble are calculated as
134 follows. For an ensemble of size N , 10^4 bootstrapped ensembles are created consisting of N
135 members each by resampling with replacement whole ensemble members from the original N -
136 member ensemble. Whole timeseries are sampled to preserve their temporal structure. The given
137 quantity is calculated for each of the 10^4 bootstrapped ensembles and confidence intervals are
138 computed from the spread in the bootstrapped estimates of the quantity.

139

140 **3 Results**

141 3.1 Model evaluation

142 We first evaluate the NAO-precipitation relationship in the MMLEA models. Overall,
143 there is a high spatial correlation between the modelled and observed NAO-precipitation patterns
144 (Figure S1a). Generally, the simulated relationship is too weak in regions where the observed
145 relationship is strongest (the Iberian Peninsula, northwest UK, and western Norway). For some
146 individual grid-cells in these regions the observed relationship lies outside the inter-member
147 ensemble spread indicating local biases. Averaged over northern Europe, however, the observed
148 relationship falls within the inter-member spread so we cannot conclude there is any systematic
149 model bias (Figure S1b). Conversely, all models except MPI-ESM-LR are unable to simulate a
150 drying in southern Europe as large as observed for a positive NAO index anomaly.

151 Following Thompson et al. (2017), the model representation of NAO variability is
152 examined by comparing the modelled and observed distributions of historical annual winter
153 NAO index anomaly (Figure S2a). Figure S2b shows that the standard deviation of the observed
154 winter NAO distribution falls within the inter-member spread for every model except CSIRO-
155 Mk3.6 and EC-EARTH, which have too low variability. All MMLEA models have a skewness
156 and kurtosis which is indistinguishable from the observations. CSIRO-Mk3.6, however, has a
157 positive ensemble median skewness, while the observed NAO distribution has an overall

158 negative skewness, consistent with dynamic arguments showing enhanced persistence of
159 negative NAO events (Woollings et al., 2010). The MMLEA models generally simulate 5th and
160 95th percentile extreme NAO winters of a comparable magnitude to Obs LE with the exception
161 of CSIRO-Mk3.6 (Figure S2a). Considering the minimum and maximum values of the modelled
162 distributions, all models except CSIRO-Mk3.6 can reproduce NAO winters of a similar
163 magnitude to the two most negative and two most positive years for 20CRv3. On these grounds,
164 CSIRO-Mk3.6 and EC-EARTH will not be used in the results relating to extreme NAO winters
165 (Section 3.3).

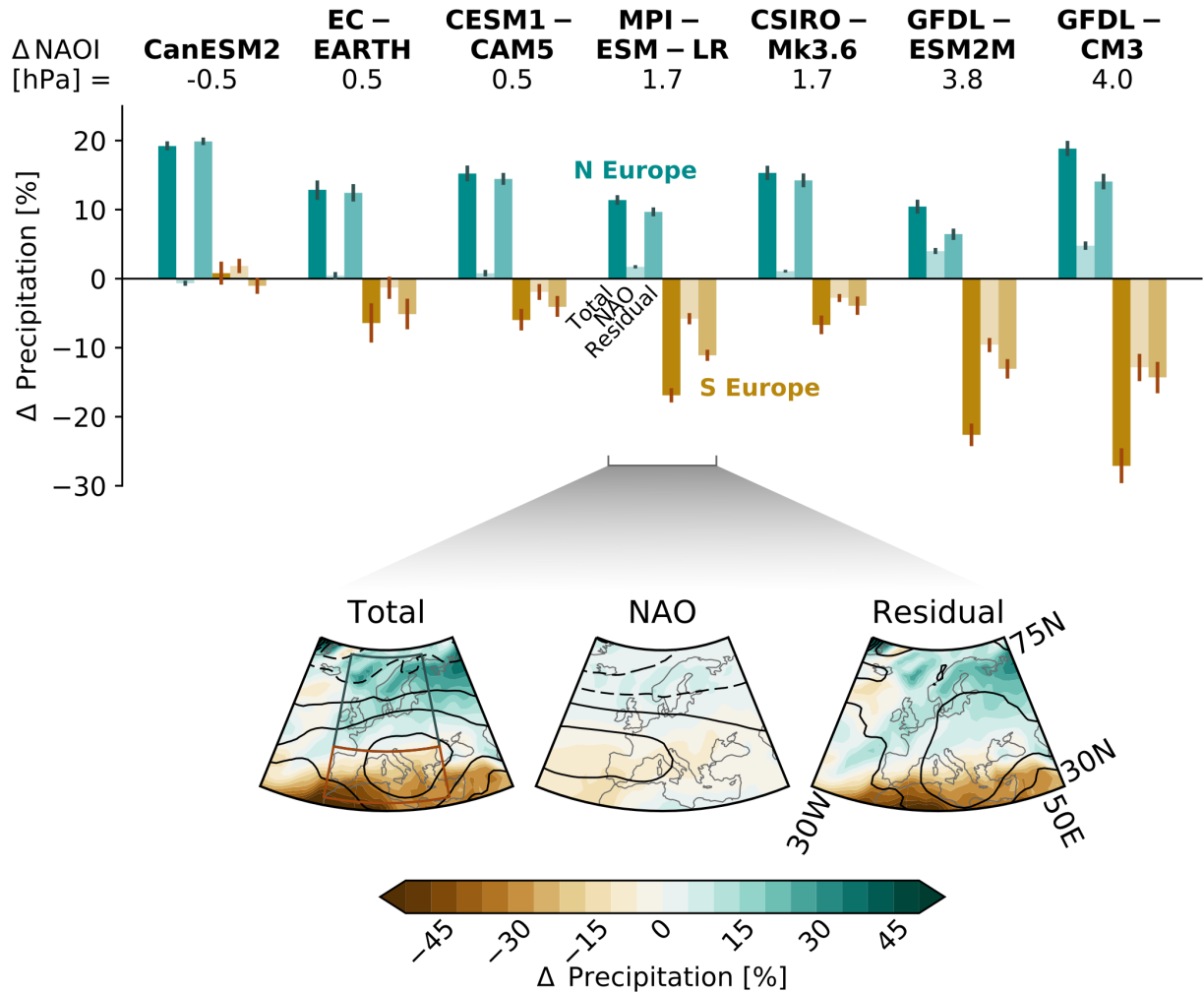
166 3.2 Role of the NAO in European mean winter precipitation projections

167 Figure 1 shows ensemble mean winter precipitation anomalies between the future (2080-
168 2099) and present-day (1995-2014) for northern and southern Europe in the MMLEA models,
169 where these are decomposed into an NAO-congruent part and a residual (Section 2.2). The
170 spatial patterns of precipitation change are generally similar across the models (Figure S3).
171 Figure 1 shows MPI-ESM-LR as an example, chosen because it lies near the centre of the
172 MMLEA and CMIP5/6 intermodel spread in projected NAO index change (McKenna &
173 Maycock, 2021). CanESM2 and the GFDL models lie towards the most negative and most
174 positive end of the NAO projections, respectively.

175 In all MMLEA models, there is a future increase in total precipitation in northern Europe,
176 which ranges from 10% to 20% of the present-day climatology. The NAO contribution is
177 generally small, but as expected depends on the magnitude of the NAO trend. Specifically, the
178 NAO contributes to almost none of the total precipitation change for models with relatively small
179 to moderate NAO trends (CanESM2, EC-EARTH, CESM1-CAM5, MPI-ESM-LR, CSIRO-
180 Mk3.6) and up to one-third for models with the strongest NAO trends (GFDL-ESM2M, GFDL-
181 CM3). The residual precipitation changes, on the other hand, are generally relatively large and
182 account for the majority of the total precipitation change in all models.

183 In southern Europe, there is a future decrease in total precipitation in most models.
184 However, there is large uncertainty across models in the magnitude, from no change in
185 CanESM2 to a decrease in precipitation of 25% in GFDL-CM3. The role of the NAO in these
186 precipitation trends is proportionately larger than for northern Europe, contributing up to

Role of NAO in DJF precipitation projections, [2080-2099] – [1995-2014]



187 **Figure 1. Role of ensemble mean DJF NAO index change (ΔNAOI) in DJF precipitation**
 188 **projections (2080-2099 minus 1995-2014) in northern and southern Europe for the**
 189 **MMLEA models.** Bars show area-average precipitation anomalies in northern (blue) and
 190 southern (brown) Europe; see lower left map. Left bar: Total precipitation anomaly; Middle bar:
 191 NAO-congruent part; Right bar: Residual. Precipitation anomalies are shown as a percentage of
 192 the 1995-2014 climatology. Error bars show bootstrapped 95% confidence intervals. Contours on
 193 maps show MSLP anomalies from -2 hPa (dashed) to 2 hPa (solid) in 1 hPa intervals.

194 one-third of the total precipitation change in models with the smallest positive NAO trends (EC-
195 EARTH, CESM1-CAM5) and up to half in models with relatively moderate to large NAO trends
196 (MPI-ESM-LR, CSIRO-Mk3.6, GFDL-ESM2M, GFDL-CM3). The residual precipitation
197 changes in southern Europe all show a drying, but only dominate over the NAO-congruent
198 precipitation change in three models (EC-EARTH, MPI-ESM-LR, GFDL-ESM2M).

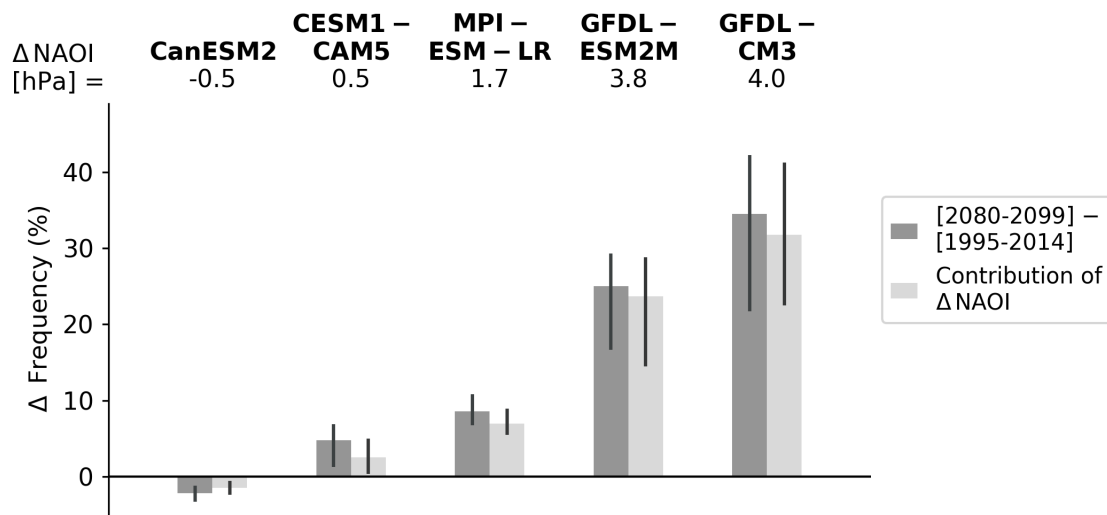
199 We now examine the NAO contribution to model uncertainty in projections of total
200 precipitation change. Similar to Fereday et al. (2018), we calculate the fractional contribution of
201 the NAO to the total intermodel variance in forced precipitation projections as $\sigma_{NAO}^2/\sigma_{TOT}^2$,
202 where $\sigma_{TOT}^2 = \sigma_{NAO}^2 + \sigma_{RES}^2$. This shows the NAO contributes around a fifth and half of the
203 intermodel spread in forced precipitation changes in northern and southern Europe, respectively.
204 For smaller regions centred on the dominant centres of action for the NAO-precipitation
205 relationship (53°N-70°N, 10°W-18°E and 36°N-44°N, 10°W-2°E; Figure S1a), the NAO
206 contributes to a larger proportion (two-thirds) of the model structural uncertainty.

207 We hypothesise the residual wetting in northern Europe mainly arises from the warming
208 climate and associated increases in specific humidity (Held & Soden, 2006; Manabe &
209 Wetherald, 1980; Trenberth et al., 2003). This is because the residual precipitation anomalies are
210 similar across the models despite different residual northern European circulation anomalies
211 (Figure S3). Furthermore, normalising the precipitation changes by changes in global mean
212 surface air temperature results in residual and total changes in northern Europe that are generally
213 similar in magnitude across the models (around 3-4 %/K and 3.5-4.5 %/K, respectively; Figure
214 S4). In contrast, this is not the case in southern Europe (Figure S4); the residual drying in the
215 Mediterranean may be associated with the residual anticyclonic circulation anomalies which are
216 not NAO-congruent (Figure S3).

217 3.3 Frequency and precipitation impacts of future extreme positive NAO winters

218 Anomalous precipitation during extreme positive NAO winters contributes to flooding in
219 northern Europe and meteorological drought in the Iberian Peninsula (Trigo et al., 2004; Zanardo
220 et al., 2019). Figure 2 shows future changes in the frequency of extreme positive NAO winters,
221 defined where the NAO index exceeds the present-day 95th percentile. The model with a negative
222 mean NAO index change (CanESM2) simulates a decrease in frequency of extreme positive

Projected change in frequency of
extreme ($\geq 95^{\text{th}}$ PC) DJF NAO+ years



223 **Figure 2: Projected change (2080-2099 minus 1995-2014) in the frequency of extreme**
 224 **positive ($\geq 95^{\text{th}}$ percentile for 1995-2014) NAO winters for selected MMLEA models (see**
 225 **Section 3.1).** Contribution of ensemble mean DJF NAO index change (ΔNAOI) is calculated by
 226 shifting the 1995-2014 distribution of annual DJF NAO index by ΔNAOI . Error bars show
 227 bootstrapped 95% confidence intervals.

228 NAO winters, while models with positive NAO index changes show increases in frequency of up
 229 to 35% (GFDL-CM3) – i.e., a 1-in-20 year winter becomes a 2-in-5 year winter. The changes in
 230 frequency can be largely explained by the ensemble mean NAO index change (Figure 2; Figure
 231 S5). While an increase in NAO variability likely contributes to part of the frequency changes in
 232 CESM1-CAM5, changes in NAO variability are not robust across MMLEA models (Figure S5).
 233 Changes in the skewness and kurtosis of the annual NAO index distribution are not robust in any
 234 model (Figure S5).

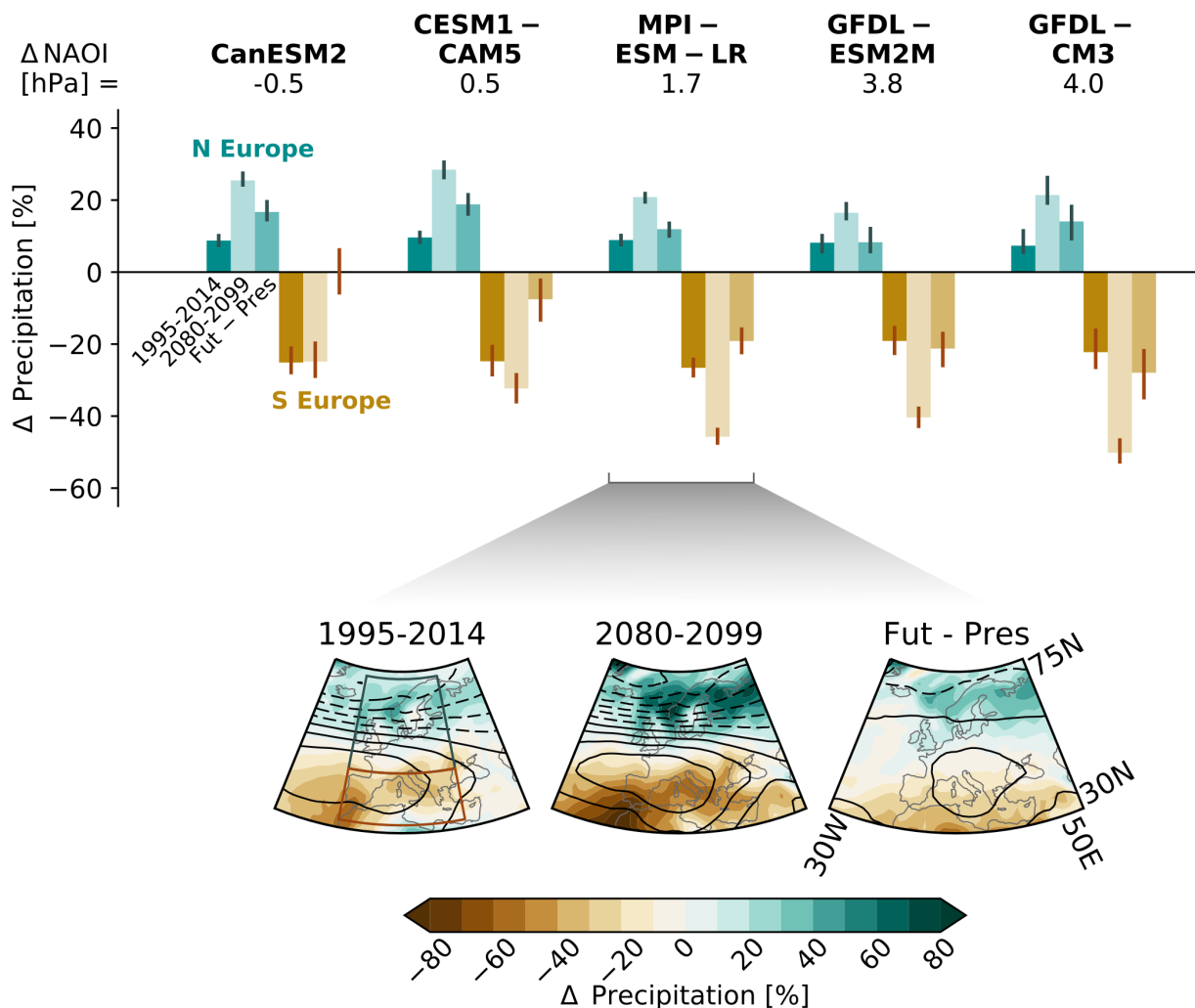
235 Figure 3 shows the future versus present-day precipitation anomalies for northern and
 236 southern Europe during extreme positive NAO winters, defined where the NAO index exceeds
 237 the 95^{th} percentile for the given period. For the present-day, extreme positive NAO winters are
 238 generally associated with 10% higher winter precipitation in northern Europe and 20% lower
 239 precipitation in southern Europe (Figure 3). In the future, all MMLEA models project an increase

240 in wet anomaly in northern Europe during extreme positive NAO winters, from two (MPI-ESM-
241 LR, GFDL-ESM2M) to three times as large (CanESM2, CESM1-CAM5, GFDL-CM3). In
242 southern Europe, models with a smaller mean NAO index change project little change in
243 precipitation (CanESM2, CESM1-CAM5), while models with a larger NAO index change
244 (GFDL-ESM2M, GFDL-CM3) project a dry anomaly during strongly positive NAO winters that
245 is around twice as large.

246 The simplest explanation for this result is that the shift in climatological mean
247 precipitation causes a shift in precipitation associated with NAO extremes. Future changes in the
248 NAO-precipitation relationship and/or NAO variability could also play a role (e.g., Deser et al.,
249 2017; Osborn, 2011).

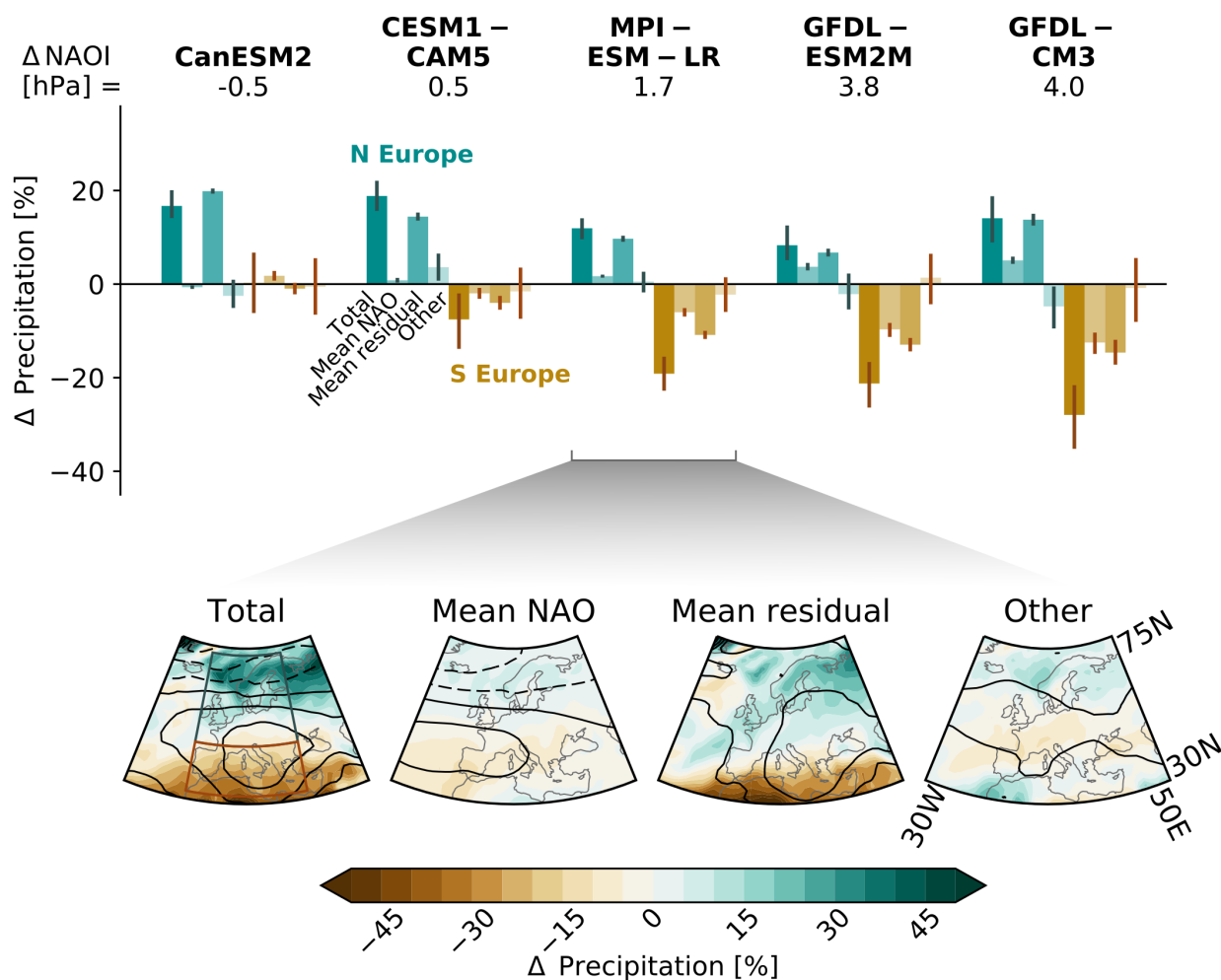
250 Figure 4 shows the future minus present-day difference in precipitation during extreme
251 positive NAO winters, decomposed into climatological mean parts and an “other” part. The
252 climatological mean changes include the part due to mean NAO index changes and a residual
253 part (i.e., the NAO-congruent part and residual from Figure 1, respectively). This shows
254 precipitation changes during extreme positive NAO winters are largely consistent with
255 climatological mean changes. In northern Europe, the increase in precipitation is dominated by
256 the mean residual changes, which – as previously discussed – are likely associated with
257 background thermodynamic effects in a warmer climate. Mean NAO changes play a larger role
258 in southern Europe than for northern Europe, contributing to around half of the total precipitation
259 anomaly in models with larger NAO index changes (GFDL-ESM2M, GFDL-CM3).

260 In CESM1-CAM5 and GFDL-CM3, there is a non-climatological increase and decrease,
261 respectively, in northern European precipitation anomaly during future extreme positive NAO
262 winters, which is different from zero within error; a sizable part of this is explained by an
263 increase and decrease in the NAO-precipitation relationship ($p < 0.05$; not shown), with small
264 contributions from an increase and decrease in interannual NAO variability (Figure S5). Changes
265 in the NAO-precipitation relationship are also responsible for the non-climatological
266 contributions in MPI-ESM-LR west of Norway and in southwestern Europe (Figure 4).
267 However, projected changes in interannual NAO variability (Figure S5) and in NAO-
268 precipitation relationship strength (not shown) are not consistent across the MMLEA models.

Precipitation anomalies in extreme ($\geq 95^{\text{th}}$ PC) DJF NAO+ years

269 **Figure 3: Precipitation anomalies in northern and southern Europe during extreme**
 270 **positive ($\geq 95^{\text{th}}$ percentile) NAO winters for 2080-2099 versus 1995-2014 in selected**
 271 **MMLEA models (see Section 3.1). Left bar: 1995-2014 anomaly; Middle bar: 2080-2099**
 272 **anomaly; Right bar: 2080-2099 anomaly minus 1995-2014 anomaly. Precipitation anomalies are**
 273 **shown as a percentage difference from the 1995-2014 winter climatology and averaged over all**
 274 **extreme positive NAO winters. Error bars show bootstrapped 95% confidence intervals. Δ NAOI**
 275 **is the ensemble mean DJF NAO index change for 2080-2099 minus 1995-2014. Contours on**
 276 **maps (see Figure S6 for all models) show MSLP anomalies from -12 hPa (dashed) to 6 hPa**
 277 **(solid) in 2 hPa intervals.**

Decomposition of precipitation projections for extreme ($\geq 95^{\text{th}}$ PC) DJF NAO+ years, [2080-2099] – [1995-2014]



278 **Figure 4: Decomposition of projected precipitation change (2080-2099 minus 1995-2014)**
 279 **during extreme positive ($\geq 95^{\text{th}}$ percentile) NAO winters in selected MMLEA models (see**
 280 **Section 3.1).** Far left bar: Total precipitation anomaly; Middle left bar: Part from ensemble mean
 281 DJF NAO index change (Δ NAOI, NAO part in Figure 1); Middle right bar: Part from ensemble
 282 mean residual change (residual in Figure 1); Far right bar: Non-climatological “other” part.
 283 Precipitation anomalies are shown as a percentage of the 1995-2014 winter climatology and
 284 averaged over all extreme positive NAO winters. Error bars show bootstrapped 95% confidence
 285 intervals. Contours on maps show MSLP anomalies from -3 hPa (dashed) to 3 hPa (solid) in 1
 286 hPa intervals.

287 **4 Discussion and Conclusions**

288 This study has examined the role of forced NAO changes for projections of winter mean
289 European precipitation using multimodel initial-condition large ensembles from the MMLEA.
290 We use this smaller multimodel ensemble because the CMIP archives typically do not provide
291 enough ensemble members to isolate forced NAO changes from internal variability (McKenna &
292 Maycock, 2021).

293 Despite the spread in late 21st century projections of the mean winter NAO index across
294 MMLEA models under the RCP8.5 scenario (McKenna & Maycock, 2021), the qualitative
295 pattern of mean winter precipitation change is very similar with wetting in northern Europe and
296 drying in southern Europe. In northern Europe, the NAO only contributes up to one-third of the
297 precipitation change in a given model and explains one-fifth of the intermodel spread. The NAO
298 plays a larger role in southern Europe, contributing up to half of the precipitation change and
299 explaining half of the intermodel spread. The residual intermodel spread in southern European
300 precipitation change may arise from spread in other aspects of atmospheric circulation change;
301 indeed, a sizable part of the spread in forced MSLP projections over southern Europe is not
302 NAO-congruent (McKenna & Maycock, 2021). The NAO is relatively more important for
303 precipitation change in certain smaller regions, including northwest Europe and the Iberian
304 Peninsula, than at a continental scale.

305 Stephenson et al. (2006) showed the NAO is not a key factor in European mean winter
306 precipitation projections for an earlier generation of climate models, where only one ensemble
307 member was available per model meaning forced changes could not be distinguished from
308 internal variability. Our analysis using MMLEA suggests Stephenson et al. (2006)'s result is
309 only robust in northern Europe. Differences in future atmospheric circulation change across the
310 CMIP5 models have been found to contribute to 75%-80% of the intermodel spread in
311 projections of mean winter precipitation in southern Europe or the Mediterranean (Fereday et al.,
312 2018; Zappa et al., 2015). The results presented here suggest a large part of the forced
313 component of this spread could be reduced through improved understanding of the NAO.

314 Second, we examine future changes in the frequency of extreme (1-in-20 year) positive
315 NAO winters, which are often associated with severe societal impacts. The MMLEA models

316 generally project an increase in extreme positive NAO winter frequency, largely due to a positive
317 shift in mean NAO index. The increase can be up to 35%, but large intermodel spread in the
318 magnitude of mean NAO index changes (McKenna & Maycock, 2021) results in large model
319 uncertainty in extreme frequency changes.

320 Third, we show extreme positive NAO winters have more severe precipitation impacts in
321 future in all MMLEA models. In particular, future extreme positive NAO winters have northern
322 European wet anomalies that are two to three times larger than in the present-day and southern
323 European dry anomalies that are up to two times larger. Mean NAO index changes contribute up
324 to half of the southern European precipitation changes. Across the MMLEA models, however,
325 the most robust Europe-wide contribution is from changes in climatological winter precipitation
326 that are unconnected with the NAO. Specifically, precipitation anomalies during future extreme
327 positive NAO winters amount to NAO-induced precipitation anomalies similar to present-day
328 superposed onto a future background climatology that constructively interferes with the NAO
329 pattern; this coincidence between mean state changes and interannual variability has implications
330 for climate adaptation and resilience to this type of seasonal extreme.

331 Multiple studies have shown increased precipitation within extratropical cyclones in a
332 warmer climate (e.g., Hawcroft et al., 2018; Kodama et al., 2019; Yettella & Kay, 2017), and
333 since the NAO is associated with changes in the position and intensity of the storm track (Hurrell
334 et al., 2003) we anticipated the NAO-precipitation relationship would strengthen in future.
335 However, such a strengthening is not robustly found in models. Further studies are required to
336 establish the connection between the cyclone-centric view of climate change and the perspective
337 of changes in large-scale circulation and storm tracks.

338 Model biases could influence this study's results. For example, the MMLEA models may
339 underestimate NAO-congruent changes in southern European precipitation given the too-weak
340 NAO-precipitation relationship in this region. They may also underestimate future increases in
341 northern European precipitation as compared to higher resolution models (Moreno-Chamarro et
342 al., 2021). Multiple Regional Climate Model initial-condition large ensembles are now becoming
343 available (Maher et al., 2021a), which could be used to further examine the influence of these
344 biases. Importantly, models have been shown to underestimate predictable forced NAO

345 variations by a factor of two on seasonal timescales (Baker et al., 2018; Dunstone et al., 2016;
346 Eade et al., 2014; Scaife & Smith, 2018; Scaife et al., 2014) and by a factor of ten on decadal
347 timescales (Smith et al., 2020). If this issue is also present in multidecadal NAO projections, the
348 NAO contribution to future changes in European winter mean precipitation may be
349 underestimated. Future work should examine whether multidecadal NAO projections have a too-
350 low signal-to-noise ratio. Understanding the dynamical mechanisms responsible for intermodel
351 spread in future forced NAO changes will also be important for identifying potential constraints
352 on the spread in southern European mean winter precipitation projections.

353

354 **Acknowledgments**

355 CMM and ACM were supported by the European Union's Horizon 2020 research and innovation
356 programme under grant agreement No 820829 (CONSTRAIN project). ACM was supported by
357 The Leverhulme Trust. We acknowledge the U.S. CLIVAR Working Group on Large Ensembles
358 for providing the MMLEA and Obs LE data, the E-OBS dataset from the EU-FP6 project
359 UERRA (<https://www.uerra.eu>) and the Copernicus Climate Change Service, and the data
360 providers in the ECA&D project (<https://www.ecad.eu>).

361

362 **Data Availability Statement**

363 The Multimodel Large Ensemble Archive and Observational Large Ensemble data can be
364 accessed at <http://www.cesm.ucar.edu/projects/community-projects/MMLEA/>. The GFDL-
365 ESM2M large ensemble data used here can be accessed from the Princeton Large Ensemble
366 Archive through Globus (<https://www.sarahschlunegger.com/large-ensemble-archive>). 20CRv3
367 can be downloaded from https://psl.noaa.gov/data/gridded/data.20thC_ReanV3.html and E-OBS
368 from https://surfobs.climate.copernicus.eu/dataaccess/access_eobs.php.

369 **References**

- 370 Álvarez-García, F. J., OrtizBevia, M. J., Cabos, W., Tasambay-Salazar, M., & RuizdeElvira, A.
371 (2019). Linear and nonlinear links of winter European precipitation to Northern
372 Hemisphere circulation patterns. *Climate Dynamics*, *52*, 6533–6555.
373 <https://doi.org/10.1007/s00382-018-4531-6>
- 374 Baker, L. H., Shaffrey, L. C., Sutton, R. T., Weisheimer, A., & Scaife, A. A. (2018). An
375 intercomparison of skill and overconfidence/underconfidence of the wintertime North
376 Atlantic Oscillation in multimodel seasonal forecasts. *Geophysical Research Letters*, *45*,
377 7808–7817. <https://doi.org/10.1029/2018GL078838>
- 378 Compo, G. P., Whitaker, J. S., Sardeshmukh, P. D., Matsui, N., Allan, R. J., Yin, X., et al.
379 (2011). The Twentieth Century Reanalysis Project. *Quarterly Journal of the Royal*
380 *Meteorological Society*, *137*(654), 1–28. <https://doi.org/10.1002/qj.776>
- 381 Cornes, R., van der Schrier, G., van den Besselaar, E. J. M., & Jones, P. D. (2018). An Ensemble
382 Version of the E-OBS Temperature and Precipitation Datasets. *Journal of Geophysical*
383 *Research: Atmospheres*, *123*(17), 9391–9409. <https://doi.org/10.1029/2017JD028200>
- 384 Deser, C., Hurrell, J. W., & Phillips, A. S. (2017). The role of the North Atlantic Oscillation in
385 European climate projections. *Climate Dynamics*, *49*, 3141–3157.
386 <https://doi.org/10.1007/s00382-016-3502-z>
- 387 Deser, C., Lehner, F., Rodgers, K. B., Ault, T., Delworth, T. L., DiNezio, P. N., et al. (2020).
388 Insights from Earth system model initial-condition large ensembles and future prospects.
389 *Nature Climate Change*, *10*, 277–286. <https://doi.org/10.1038/s41558-020-0731-2>
- 390 Deser, C., Phillips, A., Bourdette, V., & Teng, H. (2012). Uncertainty in climate change
391 projections: the role of internal variability. *Climate Dynamics*, *38*, 527–546.
392 <https://doi.org/10.1007/s00382-010-0977-x>
- 393 Douville, H., Raghavan, K., Renwick, J., Allan, R. P., Arias, P. A., Barlow, M., et al. (2021).
394 Water Cycle Changes. In Masson-Delmotte, V., et al. (Eds.), *Climate Change 2021: The*
395 *Physical Science Basis. Contribution of Working Group I to the Sixth Assessment Report*

- 396 *of the Intergovernmental Panel on Climate Change*. Cambridge, UK: Cambridge
397 University Press. In Press.
- 398 Dunstone, N., Smith, D., Scaife, A., Hermanson, L., Eade, R., Robinson, N., et al. (2016). Skilful
399 predictions of the winter North Atlantic Oscillation one year ahead. *Nature Geoscience*,
400 9, 809–814. <https://doi.org/10.1038/ngeo2824>
- 401 Eade, R., Smith, D., Scaife, A., Wallace, E., Dunstone, N., Hermanson, L., & Robinson, N.
402 (2014). Do seasonal-to-decadal climate predictions underestimate the predictability of the
403 real world? *Geophysical Research Letters*, 41(15), 5620–5628.
404 <https://doi.org/10.1002/2014GL061146>
- 405 Fereday, D., Chadwick, R., Knight, J., & Scaife, A. A. (2018). Atmospheric Dynamics is the
406 Largest Source of Uncertainty in Future Winter European Rainfall. *Journal of Climate*,
407 31(3), 963–977. <https://doi.org/10.1175/JCLI-D-17-0048.1>
- 408 Hawcroft, M., Walsh, E., Hodges, K., & Zappa, G. (2018). Significantly increased extreme
409 precipitation expected in Europe and North America from extratropical cyclones.
410 *Environmental Research Letters*, 13(12), 124006. [https://doi.org/10.1088/1748-
411 9326/aaed59](https://doi.org/10.1088/1748-9326/aaed59)
- 412 Hazeleger, W., Severijns, C., Semmler, T., Ștefănescu, S., Yang, S., Wang, X., et al. (2010). EC-
413 Earth. *Bulletin of the American Meteorological Society*, 91(10), 1357–1364.
414 <https://doi.org/10.1175/2010BAMS2877.1>
- 415 Held, I. M., & Soden, B. J. (2006). Robust Responses of the Hydrological Cycle to Global
416 Warming. *Journal of Climate*, 19(21), 5686–5699. <https://doi.org/10.1175/JCLI3990.1>
- 417 Hurrell, J. W., Kushnir, Y., Ottersen, G., & Visbeck, M. (2003). An overview of the North
418 Atlantic Oscillation. In J. W. Hurrell, Y., et al. (Eds.), *The North Atlantic Oscillation:
419 Climate Significance and Environmental Impact, Geophysical Monograph Series* (Vol.
420 134, pp. 1–35). Washington, DC: American Geophysical Union.
421 <https://doi.org/10.1029/134GM01>

- 422 Jeffrey, S., Rotstayn, L., Collier, M., Dravitzki, S., Hamalainen, C., Moeseneder, C., et al.
423 (2013). Australia's CMIP5 submission using the CSIRO-Mk3.6 model. *Australian*
424 *Meteorological and Oceanographic Journal*, 63(1), 1–14.
425 <https://doi.org/10.22499/2.6301.001>
- 426 Kay, J. E., Deser, C., Phillips, A., Mai, A., Hannay, C., Strand, G., et al. (2015). The Community
427 Earth System Model (CESM) Large Ensemble project: A community resource for
428 studying climate change in the presence of internal climate variability. *Bulletin of the*
429 *American Meteorological Society*, 96(8), 1333–1349. [https://doi.org/10.1175/BAMS-D-](https://doi.org/10.1175/BAMS-D-13-00255.1)
430 [13-00255.1](https://doi.org/10.1175/BAMS-D-13-00255.1)
- 431 Kirchmeier-Young, M. C., Zwiers, F. W., & Gillett, N. P. (2017). Attribution of extreme events
432 in Arctic sea ice extent. *Journal of Climate*, 30(2), 553–571.
433 <https://doi.org/10.1175/JCLI-D-16-0412.1>
- 434 Kodama, C., Stevens, B., Mauritsen, T., Seiki, T., & Satoh, M. (2019). A New Perspective for
435 Future Precipitation Change from Intense Extratropical Cyclones. *Geophysical Research*
436 *Letters*, 46(21), 12435–12444. <https://doi.org/10.1029/2019GL084001>
- 437 Lee, J. -Y., Marotzke, J., Bala, G., Cao, L., Corti, S., Dunne, J. P., et al. (2021). Future Global
438 Climate: Scenario-Based Projections and Near-Term Information. In Masson-Delmotte,
439 V., et al. (Eds.), *Climate Change 2021: The Physical Science Basis. Contribution of*
440 *Working Group I to the Sixth Assessment Report of the Intergovernmental Panel on*
441 *Climate Change*. Cambridge, UK: Cambridge University Press. In Press.
- 442 Maher, N., Milinski, S., & Ludwig, R. (2021a). Large ensemble climate model simulations:
443 introduction, overview, and future prospects for utilising multiple types of large
444 ensemble. *Earth System Dynamics*, 12, 401–418. [https://doi.org/10.5194/esd-12-401-](https://doi.org/10.5194/esd-12-401-2021)
445 [2021](https://doi.org/10.5194/esd-12-401-2021)
- 446 Maher, N., Milinski, S., Suarez-Gutierrez, L., Botzet, M., Dobrynin, M., Kornblueh, L., et al.
447 (2019). The Max Planck Institute Grand Ensemble: Enabling the exploration of climate
448 system variability. *Journal of Advances in Modeling Earth Systems*, 11(7), 2050–2069.
449 <https://doi.org/10.1029/2019MS001639>

- 450 Maher, N., Power, S. B., & Marotzke, J. (2021b). More accurate quantification of model-to-
451 model agreement in externally forced climatic responses over the coming century. *Nature*
452 *Communications*, 12, 788. <https://doi.org/10.1038/s41467-020-20635-w>
- 453 Manabe, S., & Wetherald, R. T. (1980). On the Distribution of Climate Change Resulting from
454 an Increase in CO₂ Content of the Atmosphere. *Journal of Atmospheric Sciences*, 37(1),
455 99–118. [https://doi.org/10.1175/1520-0469\(1980\)037<0099:OTDOCC>2.0.CO;2](https://doi.org/10.1175/1520-0469(1980)037<0099:OTDOCC>2.0.CO;2)
- 456 McKenna, C. M., & Maycock, A. C. (2021). Sources of uncertainty in Multimodel Large
457 Ensemble projections of the winter North Atlantic Oscillation. *Geophysical Research*
458 *Letters*, 48(14), e2021GL093258. <https://doi.org/10.1029/2021GL093258>
- 459 McKinnon, K. A., & Deser, C. (2018). Internal variability and regional climate trends in an
460 observational large ensemble. *Journal of Climate*, 31(17), 6783–6802.
461 <https://doi.org/10.1175/JCLI-D-17-0901.1>
- 462 Moreno-Chamarro, E., Caron, L. P., Ortega, P., Tomas, S. L., & Roberts, M. J. (2021). Can we
463 trust CMIP5/6 future projections of European winter precipitation? *Environmental*
464 *Research Letters*, 16(5), 054063. <https://doi.org/10.1088/1748-9326/abf28a>
- 465 Osborn T. J. (2011). Variability and Changes in the North Atlantic Oscillation Index. In Vicente-
466 Serrano S., Trigo R. (Eds.), *Hydrological, Socioeconomic and Ecological Impacts of the*
467 *North Atlantic Oscillation in the Mediterranean Region. Advances in Global Change*
468 *Research* (Vol. 46, pp. 9–22). Dordrecht, Netherlands: Springer.
469 https://doi.org/10.1007/978-94-007-1372-7_2
- 470 Qian, B., Corte-Real, J., & Xu, H. (2000). Is the North Atlantic Oscillation the most important
471 atmospheric pattern for precipitation in Europe? *Journal of Geophysical Research:*
472 *Atmospheres*, 105(D9), 11901–11910. <https://doi.org/10.1029/2000JD900102>
- 473 Roberts, M. J., Baker, A., Blockley, E. W., Calvert, D., Coward, A., Hewitt, H. T., et al. (2019).
474 Description of the resolution hierarchy of the global coupled HadGEM3-GC3.1 model as
475 used in CMIP6 HighResMIP experiments. *Geoscientific Model Developments*, 12(12),
476 4999–5028. <https://doi.org/10.5194/gmd-12-4999-2019>

- 477 Rodgers, K. B., Lin, J., & Frölicher, T. L. (2015). Emergence of multiple ocean ecosystem
478 drivers in a large ensemble suite with an Earth system model. *Biogeosciences*, *12*(11),
479 3301–3320. <https://doi.org/10.5194/bg-12-3301-2015>
- 480 Scaife, A. A., Arribas, A., Blockley, E., Brookshaw, A., Clark, R. T., Dunstone, N., et al. (2014).
481 Skillful long-range prediction of European and North American winters. *Geophysical*
482 *Research Letters*, *41*(7), 2514–2519. <https://doi.org/10.1002/2014GL059637>
- 483 Scaife, A. A., & Smith, D. (2018). A signal-to-noise paradox in climate science. *npj Climate and*
484 *Atmospheric Science*, *1*, 28. <https://doi.org/10.1038/s41612-018-0038-4>
- 485 Schlunegger, S., Rodgers, K. B., Sarmiento, J. L., Frölicher, T. L., Dunne, J. P., Ishii, M., &
486 Slater, R. (2019). Emergence of anthropogenic signals in the ocean carbon cycle. *Nature*
487 *Climate Change*, *9*, 719–725. <https://doi.org/10.1038/s41558-019-0553-2>
- 488 Schulzweida, Uwe. (2021). CDO User Guide (Version 2.0.0). Zenodo.
489 <http://doi.org/10.5281/zenodo.5614769>
- 490 Seager, R., Liu, H., Henderson, N., Simpson, I., Kelley, C., Shaw, T., et al. (2014). Causes of
491 Increasing Aridification of the Mediterranean Region in Response to Rising Greenhouse
492 Gases. *Journal of Climate*, *27*(12), 4655–4676. [https://doi.org/10.1175/JCLI-D-13-](https://doi.org/10.1175/JCLI-D-13-00446.1)
493 [00446.1](https://doi.org/10.1175/JCLI-D-13-00446.1)
- 494 Seager, R., Liu, H., Kushnir, Y., Osborn, T. J., Simpson, I. R., Kelley, C. R., & Nakamura, J.
495 (2020). Mechanisms of Winter Precipitation Variability in the European–Mediterranean
496 Region Associated with the North Atlantic Oscillation. *Journal of Climate*, *33*(16), 7179–
497 7196. <https://doi.org/10.1175/JCLI-D-20-0011.1>
- 498 Seager, R., Naik, N., & Vecchi, G. A. (2010). Thermodynamic and Dynamic Mechanisms for
499 Large-Scale Changes in the Hydrological Cycle in Response to Global Warming. *Journal*
500 *of Climate*, *23*(17), 4651–4668. <https://doi.org/10.1175/2010JCLI3655.1>
- 501 Shepherd, T. (2014). Atmospheric circulation as a source of uncertainty in climate change
502 projections. *Nature Geoscience*, *7*, 703–708. <https://doi.org/10.1038/ngeo2253>

- 503 Slivinski, L. C., Compo, G. P., Whitaker, J. S., Sardeshmukh, P. D., Giese, B. S., McColl, C., et
504 al. (2019). Towards a more reliable historical reanalysis: Improvements for version 3 of
505 the Twentieth Century Reanalysis system. *Quarterly Journal of the Royal Meteorological*
506 *Society*, 145(724), 2876–2908. <https://doi.org/10.1002/qj.3598>
- 507 Smith, D. M., Scaife, A. A., Eade, R., Athanasiadis, P., Bellucci, A., Bethke, I., et al. (2020).
508 North Atlantic climate far more predictable than models imply. *Nature*, 583, 796–800.
509 <https://doi.org/10.1038/s41586-020-2525-0>
- 510 Stephenson, D., Pavan, V., Collins, M., Junge, M., Quadrelli, R., & Participating CMIP2
511 Modelling Groups (2006). North Atlantic Oscillation response to transient greenhouse
512 gas forcing and the impact on European winter climate: A CMIP2 multi-model
513 assessment. *Climate Dynamics*, 27(4), 401–420. [https://doi.org/10.1007/s00382-006-](https://doi.org/10.1007/s00382-006-0140-x)
514 [0140-x](https://doi.org/10.1007/s00382-006-0140-x)
- 515 Sun, L., Alexander, M., & Deser, C. (2018). Evolution of the global coupled climate response to
516 Arctic Sea ice loss during 1990–2090 and its contribution to climate change. *Journal of*
517 *Climate*, 31(19), 7823–7843. <https://doi.org/10.1175/JCLI-D-18-0134.1>
- 518 Thompson, V., Dunstone, N. J., Scaife, A. A., Smith, D. M., Slingo, J. M., Brown, S., & Belcher,
519 S. E. (2017). High risk of unprecedented UK rainfall in the current climate. *Nature*
520 *Communications*, 8, 107. <https://doi.org/10.1038/s41467-017-00275-3>
- 521 Trenberth, K. E., Dai, A., Rasmussen, R. M., & Parsons, D. B. (2003). The Changing Character
522 of Precipitation. *Bulletin of the American Meteorological Society*, 84(9), 1205–1218.
523 <https://doi.org/10.1175/BAMS-84-9-1205>
- 524 Trigo, R. M., Pozo-Vázquez, D., Osborn, T. J., Castro-Díez, Y., Gámiz-Fortis, S., & Esteban-
525 Parra, M. J. (2004). North Atlantic Oscillation influence on precipitation, river flow and
526 water resources in the Iberian Peninsula. *International Journal of Climatology*, 24(8),
527 925–944. <https://doi.org/10.1002/joc.1048>

- 528 Woollings, T., Hannachi, A., Hoskins, B., & Turner, A. (2010). A Regime View of the North
529 Atlantic Oscillation and Its Response to Anthropogenic Forcing. *Journal of Climate*,
530 23(6), 1291–1307. <https://doi.org/10.1175/2009JCLI3087.1>
- 531 Yettella, V., & Kay, J. E. (2017). How will precipitation change in extratropical cyclones as the
532 planet warms? Insights from a large initial condition climate model ensemble. *Climate*
533 *Dynamics*, 49, 1765–1781. <https://doi.org/10.1007/s00382-016-3410-2>
- 534 Zanardo, S., Nicotina, L., Hilberts, A. G. J., & Jewson, S. P. (2019). Modulation of economic
535 losses from European floods by the North Atlantic Oscillation. *Geophysical Research*
536 *Letters*, 46(5), 2563–2572. <https://doi.org/10.1029/2019GL081956>
- 537 Zappa, G., Hoskins, B. J., & Shepherd, T. G. (2015). The dependence of wintertime
538 Mediterranean precipitation on the atmospheric circulation response to climate change.
539 *Environmental Research Letters*, 10(10), 104012. [https://doi.org/10.1088/1748-
540 9326/10/10/104012](https://doi.org/10.1088/1748-9326/10/10/104012)
- 541 Zveryaev, I. I. (2006). Seasonally varying modes in long-term variability of European
542 precipitation during the 20th century. *Journal of Geophysical Research*, 111, D21116.
543 <https://doi.org/10.1029/2005JD006821>